

Effect of amino acids containing sulfur on the corrosion of mild steel in phosphoric acid solutions containing Cl^- , F^- and Fe^{3+} ions: Behavior under polarization conditions

M.S. MORAD

Electrochemistry Research Laboratory, Department of Chemistry, Faculty of Science, Assiut University, Assiut, 71516, Egypt
e-mail: morad60@acc.aun.edu.eg

Received 17 August 2004; accepted in revised form 15 March 2005

Key words: amino acids, adsorption, EIS, inhibitors, mild steel, phosphoric acid corrosion

Abstract

The effect of cysteine (RSH), methionine (CH_3SR), cystine (RSSR) and *N*-acetylcysteine (ACC) on the corrosion behavior of mild steel in 40% H_3PO_4 solution without and with Cl^- , F^- , Fe^{3+} and their ternary mixtures was studied using both potentiostatic and electrochemical impedance (EIS) techniques under anodic and cathodic polarization conditions. The inorganic additives stimulate the overall corrosion reaction while the amino acids inhibit it with a predominant effect on the dissolution of iron. Both RSH and ACC are adsorbed according to Temkin's isotherm while adsorption of RSSR and CH_3SR follows Frumkin and Langmuir isotherms respectively. The standard free energy of adsorption ($\Delta G_{\text{ads}}^{\circ}$) was found to be in the order: RSSR > RSH \cong ACC > CH_3SR . The binary mixtures of Cl^- or F^- with RSH or CH_3SR are the best inhibitors (IE > 90%) while those containing ferric ions or blend I and amino acids are not good corrosion inhibitors. EIS measurements showed that the cathodic reaction, hydrogen evolution, is charge transfer controlled while the anodic one, iron dissolution, is a complex process.

1. Introduction

Trends in environmental protection and ecological aspects of the use of chemicals have changed the traditional approach to corrosion inhibition. Changes in formulation of corrosion inhibitors have been prompted primarily by an increasing demand for reduced environmental impact in discharge of industrial effluents. The limitation of the use of many organic and inorganic corrosion inhibitors because of their probable toxic effect (during or after use) or of their low efficiency under certain conditions prompts the need to investigate new substances as corrosion inhibitors.

Among the non-toxic chemicals tested as efficient inhibitors are *N*-arylpyrroles for zinc [1] and Al [2] in acid solutions, imidazole derivatives, linear sodium heptanoate and some Schiff bases for copper [3–5], blends of calcium gluconate/sodium benzoate, SAHMT, fatty acid triazoles and rare earth cinnamate compounds for steel [6–9] and benzimidazole derivatives for iron in acid solution [10]. Amino acids have been successfully used as corrosion inhibitors in many practical applications [11–20]. Little work appears to have been done on the inhibition of steel corrosion in H_3PO_4 particularly at high concentrations. Khamis et al. [21] studied the effect of some thiosemicarbazones on the corrosion of steel in

phosphoric acid produced by the wet process. They found that cinnamaldehyde thiosemicarbazone (CTSCN) is the best of the studied compounds with an inhibition efficiency up to 99% at 1×10^{-4} M.

In the first part of this work [20], the effect of amino acids containing sulfur on the corrosion behavior of mild steel in phosphoric acid solutions containing Cl^- , F^- and Fe^{3+} ions was studied near and at the corrosion potential using both linear polarization resistance and electrochemical impedance techniques (at the corrosion potential). The present work studies the influence of cysteine (RSH), methionine (CH_3SR), cystine (RSSR) and *N*-acetylcysteine (ACC) on the corrosion behavior of mild steel in 40% H_3PO_4 solutions containing Cl^- , F^- and Fe^{3+} ions using potentiostatic polarization technique (Tafel plots) and electrochemical impedance spectroscopy (EIS) at different potentials.

2. Experimental

Details of the mild steel composition, preparation and the cell used were given elsewhere [13]. Measurements were performed using an EG&G Princeton Applied Research Potentiostat/Galvanostat (PAR model 273). This was monitored by an IBM personal computer via a

GBIP-IIA interface. Corrosion software M352 was used for collecting and evaluating the experimental data. Prior to the electrochemical experiment, the steel specimen was allowed to stabilize in the solution for 15 min. Potentiostatic anodic and cathodic polarization runs were conducted in the range -200 to 150 mV from the corrosion potential (E_{corr}) at a scan rate of 0.2 mV s^{-1} . Details concerning preparation of the corrosive medium, additives and other experimental conditions were given elsewhere [20]. Impedance spectra were recorded at two DC potentials, namely, -100 mV and $+30$ mV with respect to E_{corr} under the same conditions as previously reported [20]. Sulfur-containing amino acids were used in the concentration range 0.01 – 50 mM while a concentration of 10 mM was used for the blends of amino acids and the inorganic additives. The formulations of the mixtures are as follows: Blend I = $\text{Cl}^-/\text{F}^-/\text{Fe}^{3+}$, Blend II = Blend I + RSH, Blend III = Blend I + CH_3SR , Blend IV = Blend I + RSSR and Blend V = Blend I + ACC.

3. Results and discussion

3.1. Corrosion behavior in presence of Cl^- , F^- and Fe^{3+} ions

Figure 1a shows the anodic and cathodic polarization curves obtained for mild steel in 40% H_3PO_4 solution without and with 10 mM Cl^- , F^- , Fe^{3+} and blend I (10 mM for each component). The electrochemical parameters associated with these curves are given in Table 1. Values of the corrosion current densities (I_{corr}) obtained from the intersection of the anodic and cathodic branches of the polarization curve at E_{corr} are much higher in the presence of the additives than in the pure medium indicating the accelerating effect of these ions, although there is a shift of the anodic curve for the case of blend I towards lower current density (cd) values. Inspection of the polarization curves of Figure 1(a) gave rise to approximate parallel Tafel lines indicating that the presence of the additives does not modify the mechanism of the proton discharge or the iron dissolution reactions.

3.2. Corrosion behavior in presence of S-containing amino acids

Among the investigated amino acids, ACC was chosen as a representative example. Figure 1(b) shows the influence of ACC on the anodic and cathodic polarization curves of mild steel in 40% H_3PO_4 solution. The corrosion parameters deduced from these curves are given in Table 1. These results indicate that ACC inhibits the corrosion of mild steel even at the lowest examined concentration (0.01 mM). The maximum inhibition efficiency (IE%) is obtained at 1 mM concentration and remains almost constant above this concentration. Figure 1(b) shows that both the anodic

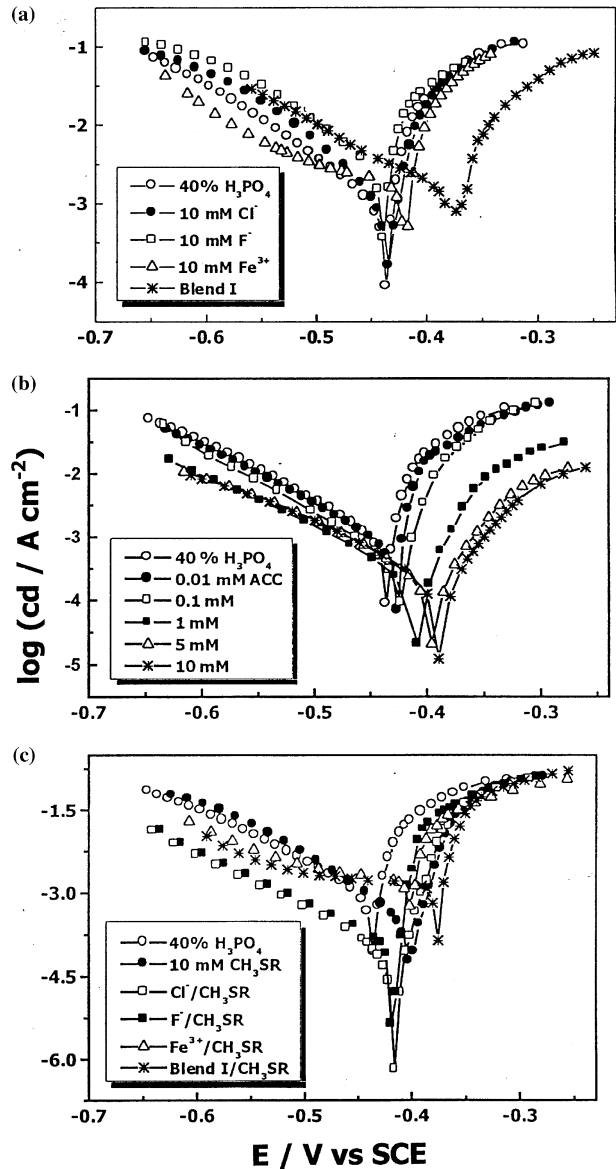


Fig. 1. Polarization curves of the system: mild steel/ H_3PO_4 without and with: (a) Inorganic additives (b) ACC (c) Mixtures of inorganic additives with CH_3SR .

and cathodic branches of the original polarization curve are shifted towards lower current densities and the anodic branch is much more affected than the cathodic

Table 1. Effect of Cl^- , F^- , Fe^{3+} and ACC on the electrochemical parameters of mild steel in H_3PO_4 solution at 40°C

Additive	$-E_{\text{corr}}/\text{mV}$	$-\beta_c^a$	β_a^a	$I_{\text{corr}}/\mu\text{A cm}^{-2}$	IE/%
0	435	119	44	1252	–
10 mM Cl^-	433	116	35	1481	18.2
10 mM F^-	438	120	51	5061	–304.2
10 mM Fe^{3+}	420	140	46	2194	–75.2
Blend I*	378	140	40	2670	–113.2
0.01 mM ACC	427	116	40	863	31.1
0.1 mM	425	111	39	553	55.8
1 mM	407	117	39	219	82.5
5 mM	395	130	51	253	79.8
10 mM	389	131	50	231	81.5

^amV/decade.

*Each mixture contains 10 mM from each component.

one. These observations indicate that ACC acts as inhibitor of mixed type with a predominant anodic effect. In the presence of RSH, RSSR and CH₃SR, the cathodic branches are shifted towards high current density values indicating the stimulation of the hydrogen evolution reaction (h.e.r.). The influence of these compounds on the original anodic polarization curve is similar to that obtained in the presence of ACC. Inhibition of the anodic reaction by the S-containing amino acids was found follow the order: ACC > RSH ≅ RSSR > CH₃SR.

Values of inhibition efficiency (IE%) presented in Table 1 were calculated from the equation :

$$IE\% = [1 - (I/I_0)] \times 100 \quad (1)$$

where I_0 and I are the corrosion current densities (calculated from extrapolation of the linear sections of the cathodic and anodic curves to the point of intersection, that is E_{corr}) without and with the additive, respectively. Values of IE% in Table 1, along with those obtained in the presence of RSH, CH₃SR and RSSR, are plotted as a function of the amino acid concentration in Figure 2. It can be observed that at 10 mM, the value of IE% reaches a maximum and remains unchanged upon further increase of additive concentration. This particular concentration was used for the next experiments.

The results of Table 1 reveal that acceleration or inhibition occur with little change in the mechanism of proton discharge reaction or anodic dissolution of iron (values of the cathodic Tafel slope β_c range from 117 to 140 mV/decade and the anodic Tafel slopes β_a range from 35 to 51 mV/decade).

3.3. Corrosion behavior in presence of inorganic ions/amino acids blends

The blends of amino acids and the inorganic additives show an effect which differs from that obtained in the presence of the individual components, that is, the blends have approximate equal inhibition effect on both anodic and cathodic reactions (mixed corrosion inhibitors). Figure 1(c) shows the effect of Cl⁻, F⁻, Fe³⁺ and

blend I with CH₃SR (representative curves). The electrochemical parameters of mild steel in H₃PO₄ solution containing Cl⁻, F⁻, Fe³⁺ with S-containing amino acids are given in Table 2. It is clearly observed that mixtures of Cl⁻ or F⁻ ions with RSH or CH₃SR are the best inhibitors (IE > 90%) while those containing Fe³⁺ or blend I with amino acids are the worst (antagonism) and a very low value (5.2%) is obtained in case of Blend III. This may be attributed to the presence of the inorganic ions may lead to the desorption of the amino acids from the electrode surface. Similar results were obtained by Ammar and Darwish [22] for the corrosion of iron in H₂SO₄ containing thiourea and NH₄SCN.

It is note worthy that the cathodic branches of the polarization curves obtained in the presence of Fe³⁺/amino acid mixtures or in the presence of the investigated blends runs over a wide range of potential parallel to the potential axis, so that the value of β_c was considered to be ∞ . This behavior is a characteristic feature for a diffusion controlled cathodic process. Similar results were obtained for the corrosion of zinc and Zn-2% Pb alloy in HCl solution containing 1×10^{-4} to 1×10^{-3} M benzo(f)-quinoline [23]. Accordingly, values of I_{corr} for these mixtures were calculated from Stern-Geary equation:

$$I_{corr} = \beta_a / 2.303 R_p \quad (2)$$

using values of R_p given elsewhere [20].

3.4. Adsorption isotherms

In order to investigate the effects of structural changes in S-containing amino acids on their ability to bind to the iron surface, the experimental data were fitted to several adsorption isotherms. The above results indicated that the amino acids do not change the mechanism of both hydrogen evolution and iron dissolution

Table 2. Electrochemical parameters of mild steel in H₃PO₄ solution containing Cl⁻, F⁻ and Fe³⁺ ions without and with S-containing amino acids

Additive concentration/mM	$-E_{corr}/mV$	$-\beta_c^a$	β_a^a	$I_{corr}/\mu A \text{ cm}^{-2}$	IE/%
0	435	119	44	1252	-
Cl ⁻ /CH ₃ SR	416	100	30	47	96.2
Cl ⁻ /RSSR	405	132	39	349	72.1
Cl ⁻ /RSH	413	100	37	122	90.2
Cl ⁻ /ACC	404	120	45	254	79.7
F ⁻ /CH ₃ SR	418	108	30	115	90.8
F ⁻ /RSSR	408	124	35	405	67.6
F ⁻ /RSH	416	100	31	78	93.7
F ⁻ /ACC	400	112	48	270	78.4
Fe ³⁺ /CH ₃ SR	400	∞	30	801	36
Fe ³⁺ /RSSR	397	∞	43	1610	-28.6
Fe ³⁺ /RSH	379	∞	38	699	44.2
Fe ³⁺ /ACC	355	∞	38	569	54.5
Blend II	395	∞	28	669	46.6
Blend III	395	∞	41	1187	5.2
Blend IV	400	∞	41	416	66.8
Blend V	371	∞	45	804	35.8

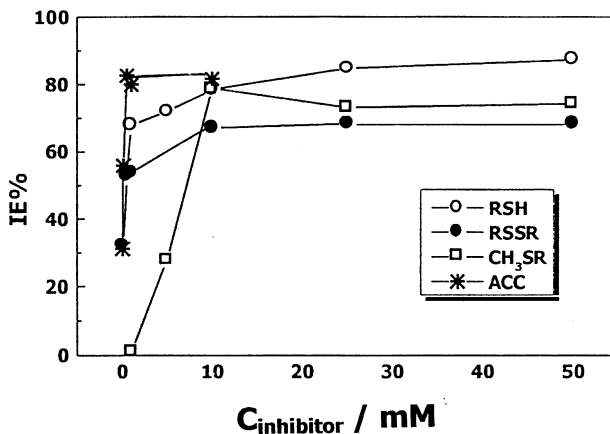


Fig. 2. Variation of IE% of amino acids with their concentrations.

^amV/decade.

reactions. So, the fraction of surface coverage θ of each inhibitor can be calculated from the equation:

$$\theta = 1 - (I/I_0) \quad (3)$$

For both RSH and ACC, the experimental data were found to fit the Temkin adsorption isotherm (Figure 3(a)), where θ varies linearly with $\log C$ (C is the molar concentration of the inhibitor) indicating mono-layer adsorption. The adsorption of RSH follows Temkin's isotherm up to 1 mM concentration after which a saturation limit is observed. Adsorption of RSSR follows Frumkin's isotherm (Figure 3(b), θ vs $\log C$ yields an S-shaped curve) with two inflections indicating bi-layer adsorption, that is, a mono-layer is adsorbed firstly followed by deposition of a second

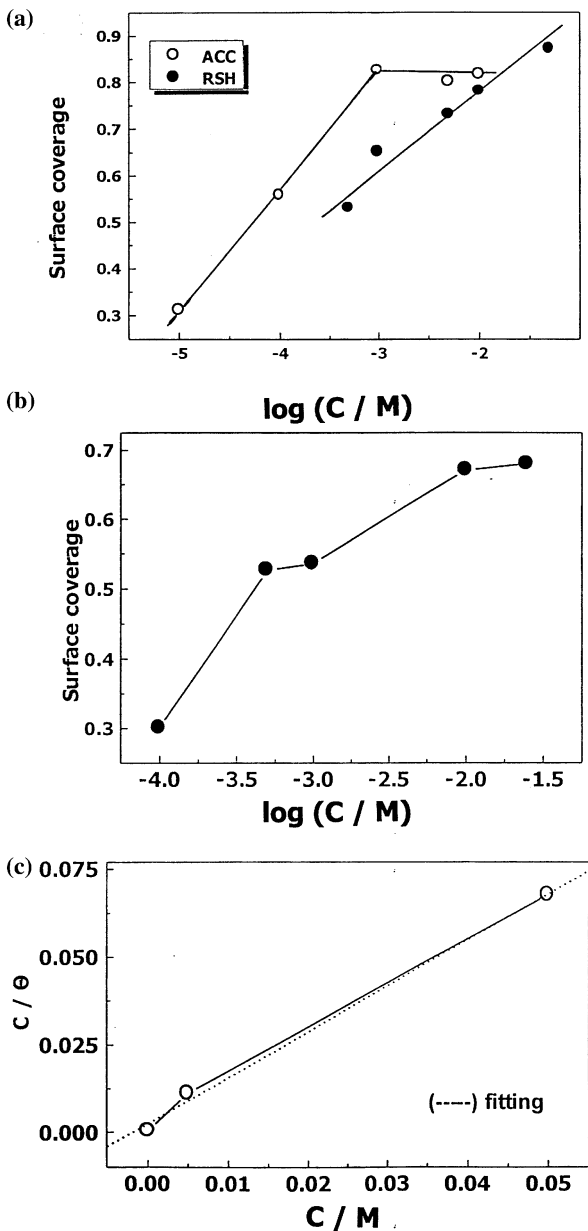


Fig. 3. Adsorption of S-containing amino acids on mild steel surface: (a) Temkin's isotherm for RSH and ACC (b) Frumkin's isotherm for CH₃SR (c) Langmuir's isotherm for RSSR.

Table 3. Parameters of adsorption of S-containing amino acids tested on mild steel in 40% H₃PO₄ solution at 40 °C

Amino acid	K_{ads}/M^{-1}	$-\Delta G_{ads}^{\circ}/kJ\ mol^{-1}$
ACC	1.6×10^6	47.61
RSH	2.15×10^6	48.4
RSSR	1.619×10^7	59.87
CH ₃ SH	2.7×10^5	42.98

layer. In the case of CH₃SR, the experimental results were found to fit the Langmuir adsorption isotherm well, as shown in Figure 3(c) (the plot of C/θ against C gives a straight line). The parameters of the adsorption process, standard free energy change ΔG_{ads}° and the

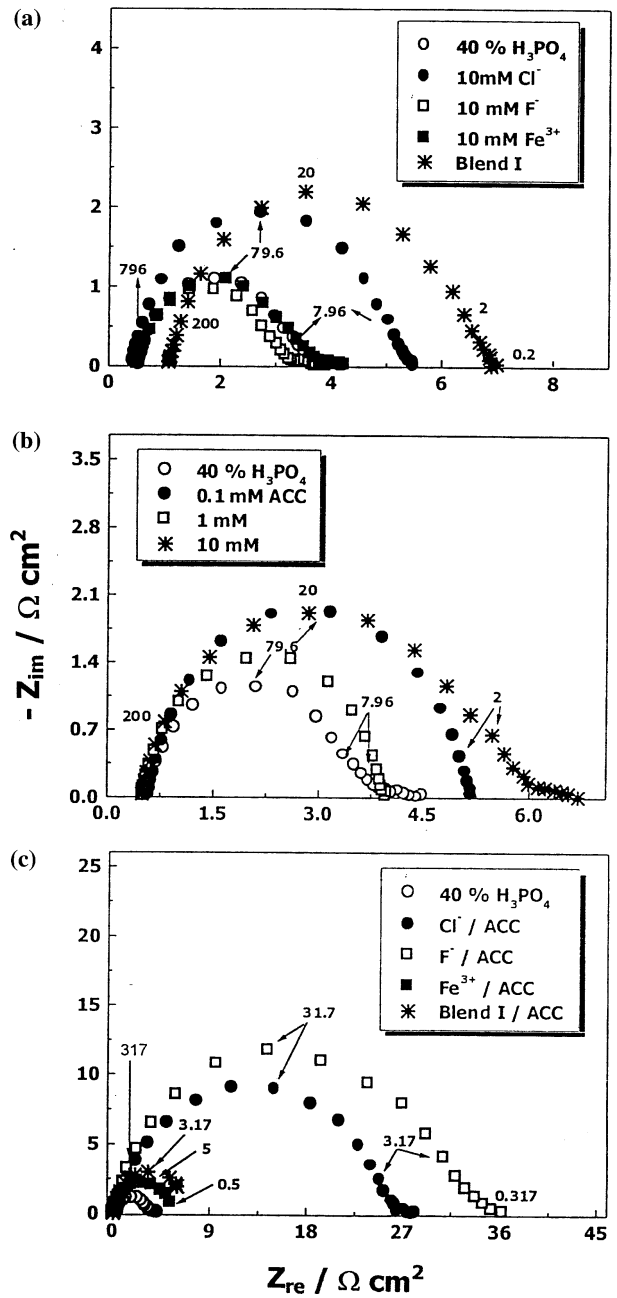


Fig. 4. Nyquist plots of mild steel corrosion obtained at -100 mV vs E_{corr} in H₃PO₄ without and with: (a) Inorganic additives (b) ACC (c) Mixtures of inorganic additives with ACC. Values in Hz.

equilibrium constant K_{ads} , were calculated and are given in Table 3. Values of both ΔG_{ads}° and K_{ads} follow the order: $RSSR > RSH \cong ACC > CH_3SR$. The large negative values of ΔG_{ads}° indicate spontaneous and efficient adsorption process. The K_{ads} value for CH_3SR is lower than those of the other amino acids indicating less adsorption of methionine. The different adsorption behavior exerted by the investigated amino acids can be ascribed to the effect of structure. All the amino acids are assumed to adsorb through the sulfur atom (the most feasible adsorption center). The presence of the acetyl group ($-COCH_3$) attached to the amino group may increase the adsorption of ACC via interaction of the oxygen of the carbonyl group with the steel surface. This may explain the higher IE% of ACC than RSH especially at low concentrations (Figure 2). In spite of the presence of the $-CH_3$ group attached to the sulfur atom in the case of methionine, the steric hindrance exerted by this group affects the stability of the adsorbed layer. The high negative value of ΔG_{ads}° indicates that the disulfide RSSR is adsorbed via the two sulfur atoms.

3.5. Impedance spectroscopy

Based on the results of the polarization curves two potential values, -100 and $+30$ mV from E_{corr} , were chosen to carry out impedance measurements. At these potentials, a remarkable difference between the corresponding values of current density was noticed in the presence of the additives. On the other hand, ACC was selected to represent the amino acids and only three concentrations namely, 0.1, 1 and 10 mM, were used.

3.5.1. EIS at -100 mV vs E_{corr}

Typical impedance diagrams (Nyquist plots) recorded for mild steel in 40% H_3PO_4 solution at -100 mV with respect to E_{corr} without and with 10 mM Cl^- , F^- , Fe^{3+} , and blend I are shown in Figure 4(a). Those obtained in the presence of ACC and mixtures of the inorganic

Table 4. Values of the charge transfer resistance, capacity of the double layer and inhibition efficiency obtained from the impedance results of the system: mild steel/ H_3PO_4 /ACC without and with Cl^- , F^- , Fe^{3+} ions and their mixtures under polarization conditions

Additive concentration/ mM	At -100 mV vs E_{corr}			At $+30$ mV vs E_{corr}	
	$R_{ct}/\Omega\text{ cm}^2$	$C_{dl}/\mu\text{F cm}^{-2}$	IE/%	$R_{ct}/\Omega\text{ cm}^2$	IE/%
0	2.84	707	—	2.1	—
10 Cl^-	4.86	411	41.6	2.4	12.5
10 F^-	2.65	754	-7.2	2.77	24.2
10 Fe^{3+}	2.96	679	4.0	2.7	22.2
Blend I *	5.6	566	49.3	2.5	16.0
0.1 ACC	4.6	435	38.2	3.1	32.2
1	3.44	561	47.4	4.5	53.3
10	5.4	370	38.3	11.4	81.5
Cl^- /ACC	25.65	195	89	12.9	83.7
F^- /ACC	32.39	155	91.2	15.9	86.8
Fe^{3+} /ACC	4.5	444	36.9	9.2	77.2
Blend I /ACC	7.2	440	60.5	14.2	85.2

additives with ACC are shown in Figure 4(b) and (c), respectively. Each spectrum consists of one capacitive loop. As the presence of the investigated additives did not substantially alter the profile of the impedance spectrum obtained in the pure acid solution, it is concluded that the mechanism of hydrogen evolution reaction is the same in the absence and presence of the additives and the charge transfer process is the slow step. Accordingly, a simple equivalent circuit consisting of parallel capacitor – resistor combination at the electrode/solution interface is assumed [24]. Among the impedance parameters calculated from fitting the semicircle, values of the charge transfer resistance (R_{ct}) and double layer capacity C_{dl} and given along with values of IE% in Table 4. The values of R_{ct} obtained in the presence of Cl^- and blend I are higher than that for the pure medium

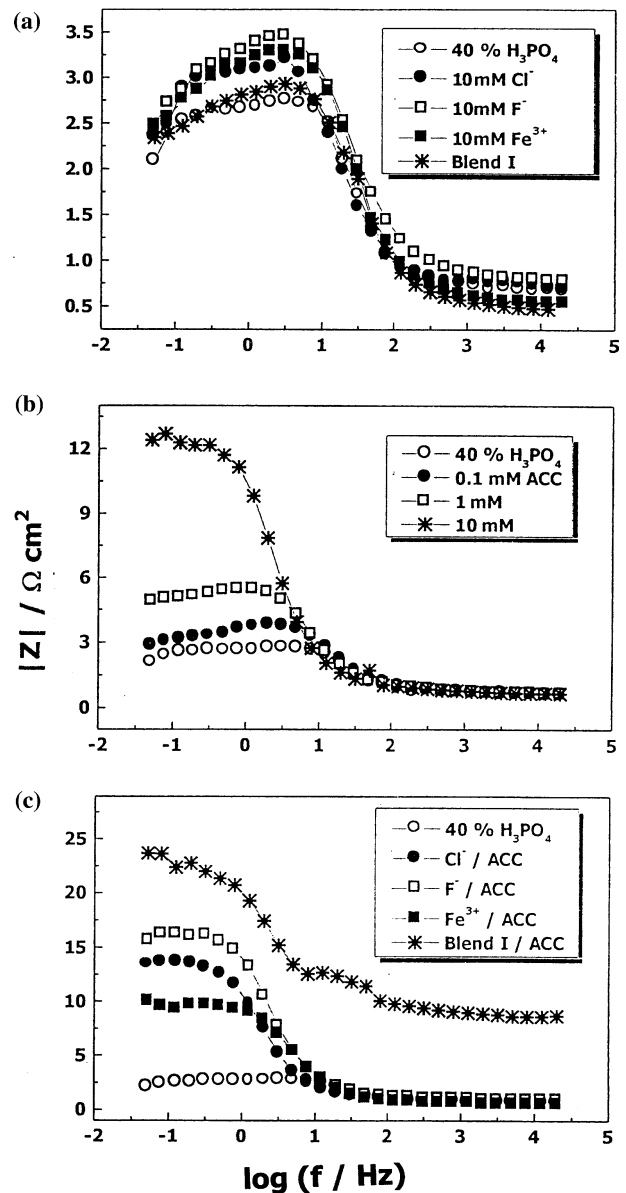


Fig. 5. Bode $|Z|/\log f$ plots of mild steel corrosion obtained at $+30$ mV vs E_{corr} in H_3PO_4 at without and with: (a) Inorganic additives (b) ACC (c) Mixtures of inorganic additives with ACC.

indicating the inhibition effect of these additives. Slight changes in the R_{ct} value of the pure medium are observed in the presence of F^- (slight acceleration) and Fe^{3+} ions (slight inhibition). The presence of 0.1–10 mM ACC reduces the value of R_{ct} obtained in the pure medium by about 17–47%. The presence of either Cl^- or F^- ions with 10 mM ACC substantially enhances the inhibition efficiency as a result of the strong synergistic action. In contrast to Cl^- and F^- , a weak synergistic effect is observed in the presence of Blend I/ACC mixture, while the presence of Fe^{3+} ions with ACC reduces the inhibition efficiency of the later compound. The results listed in Table 4 indicate that the value of C_{dl} obtained in the pure medium is $707 \mu F cm^{-2}$. Except in the presence of 10 mM F^- ion, the value of C_{dl} obtained in the pure medium was found to decrease and the maximum decrease is noticed in presence of F^-/ACC mixture ($\sim 78\%$ inhibition). The decrease in C_{dl} indicates adsorption of the additives on the electrode surface. In the presence of F^- alone, the original C_{dl} value is increased by $\sim 6\%$ indicating the cathodic reaction is slightly accelerated.

3.5.2. EIS at +30 mV vs E_{corr}

In the anodic domain (+30 mV from E_{corr}), the impedance spectra are presented in Bode $|Z| - \log f$ format and shown in Figure 5 (a–c) while values of R_{ct} deduced from fitting of the corresponding Nyquist plots (not shown) are given in Table 4. It is worth mentioning that Nyquist plots obtained in H_3PO_4 solution without and with the inorganic additives or with 0.1 and 1 mM ACC are similar to those obtained by Lendvay-Gyorik et al. [25] for iron dissolution in dilute H_2SO_4 . At high frequencies, these diagrams start with a straight line of slope of 45° and towards lower frequencies, after passing a maximum, they turn towards the real axis and form inductive loops at very low frequencies. This situation was explained in terms of the diffuse part of the double layer. In the presence of 10 mM ACC or inorganic additives/ACC mixtures, the inductive loop disappears and a small capacitive feature appears at very high frequencies, indicating a protective film on the steel surface. As these systems are complex and the analysis of the spectra is not simple, the equivalent circuit model used under cathodic polarization conditions is not suitable here and we focus only on the R_{ct} values. In all cases the additives increase the value of R_{ct} obtained in the additive-free solution and, similar to the behavior under cathodic polarization, the maximum increase is observed in the presence of F^-/ACC mixture ($\sim 87\%$ inhibition).

As a general conclusion from the impedance results obtained under the studied polarization conditions, blends of inorganic additives with 10 mM ACC are mixed corrosion inhibitors. This result agrees well with those obtained from the polarization curves.

3.6. Mechanism of corrosion inhibition

The most important prerequisites for compounds to be efficient inhibitors are that substances should form a compact barrier film, should be chemisorbed on the metal surface and have a high adsorption energy. The investigated compounds may realize some of these prerequisites although more investigation is required.

Owing to the acidity of the medium, amino acids and other compounds having a $-NH_2$ group, can not remain in solution as free bases. Therefore it is assumed that, at least in the first few minutes of contact between the metal and the solution, they exist at the interface in the cationic form [26].

Under cathodic polarization conditions the adsorption of free molecules is not likely to be favored but the protonated species are adsorbed on the electrode surface by the electrostatic attraction. The resulting physical adsorption is not sufficiently strong to impart high inhibition efficiency. This may explain the slight displacement of the cathodic branches of the polarization curves towards lower values of current density. On the other hand, the large displacement of the anodic branches of the polarization curves towards low current density values can be explained on the basis of chemisorption of neutral amino acid molecules via the sulfur atom on the anodic sites [13, 20].

The participation of the $-NH_2$ group in the adsorption process through the lone pair of electrons of the N-atom is also possible and the adsorption of amino acids via the two adsorption centers, S and N atoms, leads to strong inhibition of the anodic dissolution reaction. More details of inhibition and/or acceleration by the investigated mixtures were given elsewhere [20].

4. Conclusions

The list is

- (1) The presence of Cl^- , F^- , Fe^{3+} and their ternary mixture stimulates the corrosion of mild steel in 40% H_3PO_4 at 40 °C.
- (2) The presence of S-containing amino acids inhibits the corrosion of mild steel and they perform well as anodic corrosion inhibitors.
- (3) The adsorption behavior of S-containing amino acids can be described as follows: Both RSH and ACC are adsorbed according to Temkin's isotherm while adsorption of RSSR and CH_3SR follow Frumkin and Langmuir isotherms respectively. The standard free energy of adsorption ΔG_{ads}^0 was found to be in the order: RSSR > RSH \cong ACC > CH_3SR .
- (4) The binary mixtures of Cl^- or F^- with RSH or CH_3SR are the best inhibitors (IE > 90%) while

those containing ferric ions or blend I and amino acids are not good inhibitors.

- (5) Electrochemical impedance measurements performed under polarization conditions showed that the cathodic reaction, hydrogen evolution, is charge transfer controlled while the anodic reaction, iron dissolution, is a complex process.

References

1. E. Stupnisek-Lisac, S. Podbrscek and T. Soric, *J. Appl. Electrochem.* **24** (1994) 779.
2. M. Metikos-Hukovic, R. Babic and Z. Grubac, *J. Appl. Electrochem.* **32** (2002) 35.
3. E. Stupnisek-Lisac, A. Loncaric Bozic and I. Cafuk, *Corrosion* **54** (1998) 713.
4. E. Rocca, G. Bertrand, C. Rapin and J.C. Labrune, *J. Electroanal. Chem.* **503** (2001) 133.
5. H. Ma, S. Chen, L. Niu, S. Zhao, S. Li and D. Li, *J. Appl. Electrochem.* **32** (2002) 65.
6. O. Lahodny-Sarc, F. Kapor and K. Halle, *Werkst. Korros.* **51** (2000) 147.
7. M.A. Quraishi and D. Jamal, *Mater. Chem. Phys.* **68** (2001) 283.
8. M.A. Quraishi and F.A. Ansari, *J. Appl. Electrochem.* **33** (2003) 233.
9. F. Blin, S.G. Leary, K. Wilson, G.B. Deacon, P.C. Junk and M. Forsyth, *J. Appl. Electrochem.* **34** (2004) 591.
10. K.F. Khaled, *Electrochim. Acta* **48** (2003) 2493.
11. V. Hluchan, B.L. Wheeler and N. Hackerman, *Werkst. Korros.* **39** (1988) 512.
12. A. Aksut and S. Biligic, *Br. Corros. J.* **28** (1993) 59.
13. M.S. Abdel-Aal, M.S. Morad and Z.A. Ahmed. Proceedings of the 8th Europ. Symp. Corrosion Inhibitors, Annal. Univ. Ferrara. N. S. Suppl. No. **10** (1995) 343.
14. G.K. Gomma, *Bull. Electrochem.* **14** (1998) 456.
15. M.S. Morad. 'Inhibition and acceleration of mild steel corrosion in pickling acids' (Ph. D. Dissertation, University of Assiut 1995), p. 31.
16. A.M. Al Mayouf. *Corros. Prev. Control.* June (1996) 68.
17. R. Salghi, B. Hammouti, S. Kertit and L. Buzzi, *Bull. Electrochem.* **13** (1997) 399.
18. G. Moretti, G. Gajo, F. Guidi, G. Capobianco and G. Quartarone. Proceedings of the 9th Eur. Symp. Corros. Inhib. (9SEIC) Ann. Univ. Ferrara N. S. Suppl. **11** (2000) 699.
19. M.S. Morad and A.A. Hermas, *J. Chem. Technol. Biotechnol.* **76** (2001) 401.
20. M.S. Morad, A.A. Hermas and M.S. Abdel Aal, *J. Chem. Technol. Biotechnol.* **77** (2002) 486.
21. E. Khamis, M.A. Ameer, N.M. AlAndis and G. Al-Senani, *Corrosion* **56** (2000) 127.
22. I.A. Ammar and S. Darwish, *Corros. Sci.* **7** (1967) 579.
23. M.S. Abdel-Aal, Z.A. Ahmed and M.S. Hassan, *J. Appl. Electrochem.* **22** (1992) 1104.
24. F. Mansfeld, M.W. Kendig and W.J. Lorenz, *J. Electrochem. Soc.* **138** (1991) 2237.
25. G. Lendvay-Gyorik, L. Meszaros, G. Meszaros and B. Lengyel, *Corros. Sci.* **42** (2000) 79.
26. J.D. Talati and D.K. Ghandi, *Corros. Sci.* **23** (1983) 1315.